

# Carbon competition between fatty acids and starch during benzoin seeds maturation slows oil accumulation speed

Zihan Zhang<sup>1</sup> · Xiaojun Wang<sup>1</sup> · Ying Luo<sup>1</sup> · Fangyuan Yu<sup>1</sup>

Received: 27 July 2016 / Accepted: 12 January 2017 / Published online: 15 February 2017  
© Springer-Verlag Berlin Heidelberg 2017

## Abstract

**Key message** The carbon flow balance is shifted to starch rather than oil accumulation during benzoin seed development stage (80–120 DAF) and thereby lipid deposition speed slows down.

**Abstract** Benzoin [*Styrax tonkinensis* (Pierre) Craib ex Hartwich] is a woody oilseed species with potential value as a biofuel feedstock. However, the continuous drop in seed crude fat concentration during maturation had remained unexplained until it was investigated in this study. Seed filling began 60 days after flowering (DAF), when the hexose-to-sucrose ratio dropped, correlating with substantial morphological changes in kernels. Oil accumulated 20 days earlier than starch, as the concentrations of free fatty acid (50–70 DAF) and diacylglycerols (50–80 DAF) increased rapidly. Fatty acid synthesis slowed between 80 and 120 days, correlating with a sharp increase in the speed of starch deposition, while triacylglycerol accumulation and the profile of fatty acids remained stable. Phosphoglucose isomerase (PGI), pyruvate dehydrogenase complex (PDHC), and malate dehydrogenase (MDH) activities dropped progressively together with acetyl coenzyme carboxylase (ACCase) after 70 DAF before the reserve storage priority shifted from fatty acids to starch. PGI, PDHC, MDH, ACCase, and diglyceride acyltransferase (DAGT) activities rose again at 120 DAF, after which the speed of fatty acid accumulation increased, correlating with a 10-day

lag phase in starch accumulation. High glucose 6-phosphate dehydrogenase (G6PDH) activity was observed during oil deposition. Soluble protein continued accumulating as protease activity decreased during benzoin seed development, while the total amylase activity rose twice between 30 and 70 DAF before the ADP-glucose pyrophosphorylase activity and starch content soared high simultaneously after 70 DAF. The collective results suggest that carbon partitioning between starch and lipid accumulation occurs during benzoin kernel development and is responsible for a reduction in the rate at which total fatty acids accumulate between 80 and 120 DAF.

**Keywords** *Styrax tonkinensis* · Seed maturation · Carbon partition · Storage reserves · Lipid synthesis

## Introduction

Benzoin [*Styrax tonkinensis* (Pierre) Craib ex Hartwich], being famous in the perfumery industry for the resin extracted from the stem of this fast-growing species (Pinyopusarerk 1994), is also known for its timber (Hieu et al. 2011), medicine (Yokoyama 2004), and ornamental (Xu and Yu 2015) values. Benzoin is native to Vietnam and Laos, and is widely distributed in the southern provinces of China. In recent years, the unresolved global food and energy crisis has urged Chinese researchers to investigate the oil-rich seeds of certain woody species, and they have reached a consensus that benzoin seeds have potentials to be utilized in daily diet oil (Shi et al. 2014) and renewable diesel industry (Chen et al. 2015). Shi et al. (2013) recently reported the lipid accumulation process in *S. tonkinensis* seeds. They found that during development, the crude oil concentration on a dry weight basis kept

Communicated by E. Magel.

✉ Fangyuan Yu  
fyyu@njfu.edu.cn

<sup>1</sup> Collaborative Innovation Center of Sustainable Forestry in Southern China, College of Forest Science, Nanjing Forestry University, Jiangsu 210037, China

dropping for nearly 30 days before it rose sharply again as seeds approached maturation. However, this change was not discussed in their paper, and other seed reserve dynamics were unreported. Therefore, we were inspired to study this intriguing phenomenon. In this case, there could be two possible reasons. First, there might be an unfavorable period for lipid accumulation when its speed is slowed down, or perhaps even negative. Second, it could be a situation that the seed total oil content keeps rising constantly, but its relative concentrations reduced as other assimilates deposit at a faster speed.

The developing seed is a powerful sink, where carbon and nitrogen provided by maternal tissues transform into starch, storage protein, and lipid, and then accumulate in the embryo and/or endosperm with temporal and spatial variation. The onset of storage deposition is mainly triggered by a high sucrose-to-hexose ratio in plants, including, for example, legume (Weber et al. 1997) and *Arabidopsis thaliana* seeds (Baud et al. 2002). In oilseed species, particularly, neutral fat is preferred over starch as seed assimilate (Ohlrogge and Browse 1995; Ohlrogge and Jaworski 1997), and unlike the storage protein, carbon skeletons of those two are exclusively obtained from hexoses (Lin et al. 2006), including glucose and fructose. Over-expression of the *E.coli* ADP-glucose pyrophosphorylase (AGP) in both *Brassica napus* seeds (Boddupalli et al. 1995) and *Arabidopsis thaliana* seeds (Lin et al. 2004) resulted in the diversion of carbon partitioning between lipid and starch, and it finally leads to a massive increase in starch content and a decrease in oil content, which suggested that the carbon funneling into seed storage lipid could be drawn upon by other metabolic pathways.

Fatty acid biosynthesis in plant cells starts with the carboxylation of acetyl coenzyme A, and this substrate pool in plastids could be contributed from more than one pathway (Ohlrogge and Browse 1995). Phosphoenolpyruvate and pyruvate produced from glycolysis are the main precursors of acetyl-CoA in developing embryos of *Brassica napus* (Schwender et al. 2006; Hay and Schwender 2011), and 82% of acetyl-CoA is consumed in lipid accumulation, eliminating most of the carbon flux around the tricarboxylic acid cycle (Schwender et al. 2006). Because photosynthesis is likely to be light-limited in young embryos, the pentose phosphate pathway presumably produces reducing power for oil accumulation (Emes and Neuhaus 1997; Wakao et al. 2008).

In this study, seed reserve accumulation and associated activity of main respiratory enzymes were measured during endosperm formation and embryo development in benzoin. We were hoping to answer the following questions: (1) would there be a period when lipid synthesis slowed down during benzoin seed maturation? (2) If yes, would this be a result of the competition among different seed reserves, in

particular between starch and lipid? (3) If again yes, would enzyme activities of glycoxidation and lipid synthesis pathway shift accordingly as a result of carbon competition? Answers to those questions may help us further understand the seed lipid accumulation in *S. tonkinensis*.

## Materials and methods

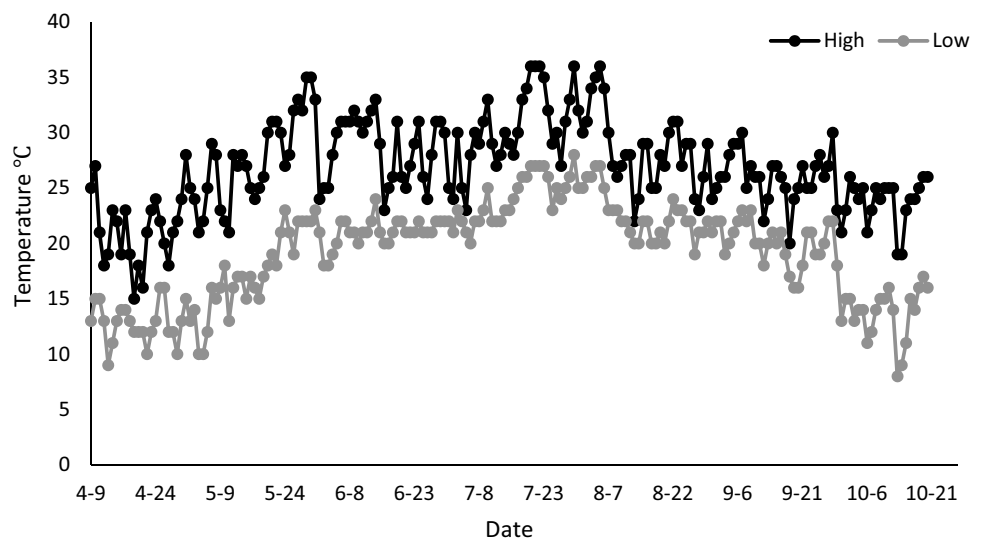
### Plant material

Two-year-old *Styrax tonkinensis* seedlings (of Jishui, Jiangxi provenance) were purchased and planted by Jiangsu Guoxing Co., Ltd., in 2011, on both sides of the Huanhu Road near the Hewangba Reservoir, Luhe District, Nanjing, China (32°54'N, 118°84'E), where they grew without fertilizer application. In late May 2014, 15 trees were tagged for sampling. The diameter at breast height (DBH), total tree height, and numbers of flowers per individual were measured (Table 1). Fresh fruits were randomly harvested in different branch directions from each selected plant from June 23rd (30 DAF) to October 11th (140 DAF), with a 9-day interval between each harvest. The high and low temperatures from the early April to late October in Luhe District were recorded (Fig. 1). Drupes were sealed in plastic bags and then embedded in an ice box before the seeds were removed and sub-sampled. Fruit collected from each developmental stage was vertically cut and photographed using a stereomicroscope. The combined parts of endosperms and embryos from 30 seeds, in four replicates each, were weighed just after they were carefully separated using a

**Table 1** Diameter at breast height (DBH), total tree height, and number of flowers per sampled *S. tonkinensis* tree

Sample tree No.	Height (m)	DBH (mm)	Flowers per tree
8	3.17	2.91	2946
9	2.94	2.60	3270
15	3.29	2.93	4472
17	3.20	3.18	7656
21	3.10	3.60	5990
27	3.26	3.69	2280
30	3.08	3.16	3216
32	2.71	2.72	2568
39	3.01	2.84	8698
40	2.82	2.64	5648
43	3.38	3.02	2402
51	3.47	2.88	1122
54	3.23	3.02	4578
68	2.52	2.15	1832
76	3.59	3.44	1936

**Fig. 1** High and low temperatures recorded at Luhe District, Nanjing, China, from April 9th to October 20th, 2014 (data acquired from the public service Website of Chinese Meteorological Administration: <http://www.weather.com.cn/>)



clean dissecting needle (FW) and after drying at 65 °C for 72 h (DW). The remaining seeds were immediately frozen in liquid nitrogen and stored at –70 °C for other analyses.

### Lipid analyses

50 de-coated seeds from each developmental stage were weighed after drying at 65 °C for 72 h. The dry kernels were then ground and the seed oil was extracted with petroleum ether (30–60 °C) using a Soxhlet apparatus, as described by Gao (2006). The flask temperature was kept at 65 °C, and the extraction lasted 24 h. Lipid was then separated from the petroleum ether using a rotary vacuum evaporator at 65 °C. After extraction, the ground seeds were weighed again, and the total crude lipid content was expressed as the percentage of oil on a dry weight basis. We failed to collect the crude oil from both 30 DAF and 40 DAF seed kernels due to insufficient dry weight and because not many seeds were left after other physiological analyses. About 0.2-mL oil was first dissolved in 2 mL of petroleum ether/benzene (1:1, v/v) and then fully mixed with 2 mL of 0.4-mol/L KOH–CH<sub>3</sub>OH to make the fatty acids methyl-esterified. Vigorous shaking was needed during a 15 min conversion at room temperature. The product was diluted with deionized water to 10 mL and the upper phase (light yellow, transparent) was analyzed by gas chromatography-mass spectrometry (GC/MS) using a TRACE DSQ GC/MS (Thermo Fisher Scientific Inc., USA). An Agilent DB-5ms capillary (30m×0.33mm×0.25 μm) column was equipped to separate different lipid compounds. The carrier gas was helium, at a flow rate of 2 mL/min. GC oven temperature was initially 60 °C for 2 min, and then gradually increased at 10 °C/min to 280 °C, which was held for 5 min. An electron ionization system was used with 70-eV ionization energy. 1 μL of the sample was injected with non-split

mode and the injector temperature was set at 260 °C. The mass spectra of eluted compounds were recorded over an *m/z* range of 33–450. To identify the oil constituents, spectra and retention times of peaks were compared in an X-caliber workstation with reference to the NIST database. An ion current peak area normalization method was used to calculate the relative amount of each component.

The extracted lipids were then transferred to a 25 mL brown-glass volumetric flask with *n*-hexane. The total lipids were fractionated by thin layer chromatography (TLC) with *n*-hexane/diethyl ether/acetic acid (80:20:1, v/v/v), as described previously (Yoshida et al. 2011). Samples were run together with the standard mixture, containing diacylglycerols (DAGs), free fatty acids (FFAs), triacylglycerols (TAGs), and phospholipids (PLs). Bands corresponding to TAGs, unknown, FFAs, 1,3-DAGs, 1,2-DAGs, and PLs were scraped into test-tubes (105×16 mm; Teflon-coated screw caps). Methyl pentadecanoate/*n*-hexane solution (20 μL; 100 mg/20 mL) was added to each tube as internal standard. Following a previously reported method (Yoshida et al. 2004), fatty acid methyl esters (FAMES) were prepared from the isolated lipid fraction and then quantified by GC/MS. Amounts of TAGs, FFAs, and DAGs were calculated using the combined FAMES peak areas by reference to the standard, and results were expressed as wt% of total FAMES (Yoshida et al. 1995).

### Carbohydrate analyses

To extract soluble sugars, 500-mg frozen de-coated seeds (for 30 and 40 DAF, 50 kernels were sub-sampled and weighed; the same below) were ground and homogenized in 8 mL deionized water. The homogenate was transferred into a test tube and kept in a boiling water bath for 20 min. After cooling to room temperature, the insoluble

residue was separated from the supernatant by centrifuging (Allegra™ X-22R, F1010 Rotor, Beckman Coulter Inc., USA; the same hereinafter) at 5000 rpm for 10 min at 15 °C. The residue was again subjected to the same extraction procedure. The combined supernatant was then diluted with deionized water and brought to a volume of 25 mL. Total soluble sugar content in each sample was measured using an anthrone colorimetric method with glucose as a standard (Li 2006). The fructose was then quantified using the method of Yu and Zhang (1999): 0.2 mL of sugar extract was mixed in a test tube with 1.4 mL deionized water and 0.4 mL resorcinol/ethanol/water (0.1:95:5, m/v/v) and placed in an 80 °C water bath for 10 min. The OD value (480 nm) was read on a spectrophotometer, using fructose as the standard. For the measurement of sucrose, the reducing sugar in 0.2 mL of extract was first neutralized with 0.1 mL NaOH (2 mol/L), and 1.4 mL 30% HCl was used to break down the sucrose into monosaccharides (and Zhang 1999). The fructose released in the mixture was then determined, and the sucrose content was calculated using the standard curve made beforehand. A kit (Shanghai RSBIO Ltd. Co., China) was used to determine the glucose content in the total soluble sugar extract, which was based on the glucose oxidase–peroxidase method. The residue remaining after sugar extraction was re-homogenized with 10 mL deionized water in a test tube. The tube was placed in boiling water and 2 mL HClO<sub>4</sub> (9.2 mol/L) was added after 15 min, followed by a further 15 min in the bath. The diluted extract was prepared by the same method used in soluble sugar extraction (see above). The starch content was calculated from a standard curve prepared using a starch solution of various concentrations. The method above was adapted from Morris (1948) and Li (2006).

#### Amino-acid and protein analyses

Kernels were homogenized in 5 mL 10% (v/v) acetic acid and then centrifuged at 5000 rpm for 10 min at 15 °C. The supernatant was diluted with deionized water to 100 mL and used for the quantification of free amino-acid content according to Rosen (1957) and following the procedure of Li (2006), with leucine as the standard. The soluble protein was quantified according to Bradford (1976). 500-mg de-coated seeds were homogenized in 5 mL extraction buffer containing 0.02-mol/L PBS (pH 7.5). After centrifuging at 6000 rpm for 20 min at 15 °C, the supernatant was diluted properly before measurement against BSA as the standard.

#### Amylase activity analysis

Amylase was assayed following the method of Bernfield (1955). For enzyme extraction, 500-mg frozen kernels from each seed developmental stage were homogenized in

8 mL deionized water at room temperature, and the mixture was centrifuged at 8,000 rpm at 4 °C for 20 min. The supernatant was used for amylase assay. The reaction system included 1 mL of 1% starch solution (1-g soluble starch dissolved in 100 mL 0.1-mol/L citrate buffer pH 5.6) and 1 mL ten times diluted supernatant, and was incubated at 40 °C for 10 min. 0.5 mL of 2-mol/L NaOH was then added to stop the enzymatic reaction. Reducing sugars were then determined by the DNS colorimetric method (Li 2006). The enzyme activity was expressed as mg sugar released per min per mg protein. The soluble protein content of the extracted supernatant was measured after Bradford (1976).

#### ADP-glucose pyrophosphorylase (AGP) activity analysis

The assay was similar to that previously described by Keller et al. (1988). AGP activity was determined by coupling the formation of glucose 1-P, to phosphoglucomutase and glucose 6-P dehydrogenase in the presence of NADP, and measuring the NADPH absorbance increase at 340 nm. A kit (Suzhou Comin Biotechnology Co., Ltd., China) was used for the enzyme extraction and measurement.

#### Protease activity analysis

To extract protease, 500-mg frozen de-coated seeds were homogenized with 5 mL 0.02-mol/L PBS pH 7.5 and then centrifuged at 8000 rpm for 20 min at 4 °C. The activity was then measured after McDonald and Chen (1965) and expressed as mg peptides liberated by the enzyme action from 2% casein solution (2-g casein in 100 mL 0.02 mol/L PBS pH 7.5) per min per mg protein. Tyrosine was used as the standard for quantification by the Folin colorimetric method of Lowry et al. (1951).

#### Glycoxidation pathway-related enzymes analyses

For the enzyme preparation, 500-mg frozen de-coated seeds were ground at 4 °C with 5 mL 0.1-mol/L Tris–HCl buffer (pH 7.4), which included 1-mmol/L EDTA-Na<sub>2</sub> and 1.5-mmol/L AsA. The homogenate was centrifuged at 12,000 rpm for 50 min at 4 °C, and the supernatant was used for malate dehydrogenase (MDH), phosphoglucose isomerase (PGI), and glucose 6-phosphate dehydrogenase (G6PDH) assays, MDH activity determination was performed with an assay kit (Nanjing Jiancheng Bioengineering Institute, China), whereby a decrease in NADH was detected by a spectrometer at 340 nm (Bergmeyer 1956). PGI and G6PDH activities were assayed by procedures provided by Brown and Wary (1968) and Simcox et al. (1979). The residue of enzyme extraction above containing pyruvate dehydrogenase complex (PDHC) was then dissolved, and the activity measurement was conducted with a kit

(Suzhou Comin Biotechnology Co., Ltd., China) based on the spectrometric method described by Ke et al. (2014).

### Acetyl coenzyme carboxylase (ACCase) and diglyceride acyltransferase (DAGT) activities analysis

ELISA (enzyme-linked immunosorbent assay) kits for analyzing the presence of ACCase and DAGT were provided by Shanghai Resun Trading Co., Ltd. The microtiter plates have been pre-coated with an antibody specific to plant ACCase (or DAGT). After antibody–antigen interactions, signals were amplified by the biotin-avidin system and the antigen targets in samples were qualified through HRP (horseradish peroxidase)–TMB (3,3',5,5'-tetramethylbenzidine) colorimetric detection system. The color change was measured spectrophotometrically at a wavelength of 450 nm. ACCase (or DAGT) concentration in samples was then determined by comparing OD value to the standard curve.

### Statistics analysis

Values were expressed as mean  $\pm$  SD of three independent experiments. Excel (Office 2013 Pro Plus, Microsoft Corporation, USA) was used to process figures. One-way analysis of variance (ANOVA) was performed using SPSS 19.0 (IBM, USA), and followed by Duncan's Multiple Range Test. *P* values less than 0.05 were considered significant within groups.

## Results

### Change of seed morphology, weight and water content

A boundary between the endosperm and the green seed coat could already be recognized under a stereomicroscope at 30 DAF (Fig. 2a). The kernel color turned milky-white, and its size was enlarged considerably by 70 DAF. Nevertheless, the differentiated axis was not seen until 80 DAF. The size of the endosperm and embryo grew gradually and filled almost the whole benzoin seed after 120 DAF.

Between 30 and 70 DAF, the fresh mass of *S. tonkinensis* seed kernels increased slowly (Fig. 2b). A dramatic change in fresh kernel weight was then observed after 70 DAF, and a 10-day lag phase appeared at 100 DAF, before the fresh matter increased again, albeit more slowly than during the former period. The combined fresh weight of endosperm and embryo reached 93.87 mg at 140 DAF. The dry kernel weight shared a similar pattern with the fresh weight, except that it increased continuously during seed development. At 140 DAF, dry kernel biomass had a 756% increase compared with that at 30 DAF. In all,

the kernel fresh and dry weight both followed a sigmoidal curve. The water content from 30 to 40 DAF remained similar, followed by a rapid and more-or-less linear decrease until 110 DAF (Fig. 2c). The water content of *S. tonkinensis* de-coated seeds remained unchanged thereafter, ranging from 25.89 to 28.33%.

### Evolution of lipids

Crude oil and total fatty acids (TFA) concentrations were analyzed to test whether TFA represents most of the crude oil in benzoin developing de-coated seeds. The lipophilic substances accounted for a large fraction (74.8%) of the crude fat at 50 DAF (Fig. 3b). Its proportion dropped quickly thereafter when the TFA content rose to more than 90% of the crude oil. Both crude oil and TFA dynamics showed an up-down-and-up pattern, and the fall was observed during 80 and 120 DAF, with a 22.66% and a 23.00% decrease respectively (Fig. 3a). In the dynamics of TFA total amount (Fig. 3c), a sharp rise could be observed between 70 and 80 DAF, with a 609% increase, after which the speed of accumulation became much slower until 120 DAF. The TFA content started to soar again before its maximum amount of 38.42 mg per de-coated seed was reached at 140 DAF. Similarly, the total TAG content remained low in the first 40 days. It then began to increase gradually until 100 DAF, when a lag phase was detected for the next 20 days. TAG synthesis rebooted during the final 20 days, reaching 67.0% of the total lipid content at 140 DAF. FFA concentration peaked twice during kernel development, with the first and higher peak (56.2%) at 70 DAF and the second and lower one (26.3%) at 120 DAF (Fig. 3d). DAG concentration shared the same changing pattern with FFA, but with two 10-day-delayed peaks at 80 and 130 DAF. ACCase activity peaked twice along with the lipid accumulation process, at 70 and 120 DAF. DAGT had a single peak at 90 DAF, but it continued to rise after 120 DAF and reached 0.56-nmol/mg protein at 140 DAF.

The young kernels contained approximately equal amounts of saturated FA (50.16%) and unsaturated FA (42.54%) at 50 DAF (Table 2). The fatty acid composition changed rapidly afterwards, with the proportion of C 16:0 (palmitic acid) and C 18:0 (stearic acid) falling markedly and tending to be unchanged after 70 DAF, while the level of C 18:1 (oleic acid) and C 18:2 (linoleic acid) climbed progressively; nevertheless, the C 18:1 fraction increased by 9.59% and the C 18:2 fraction dropped by 4.83% during the final 20 days. Other fatty acids, except for hexanoic acid, shared a similar evolving pattern, where they peaked at 120 DAF. Moreover, they only represented less than 3% of TFA accumulatively.

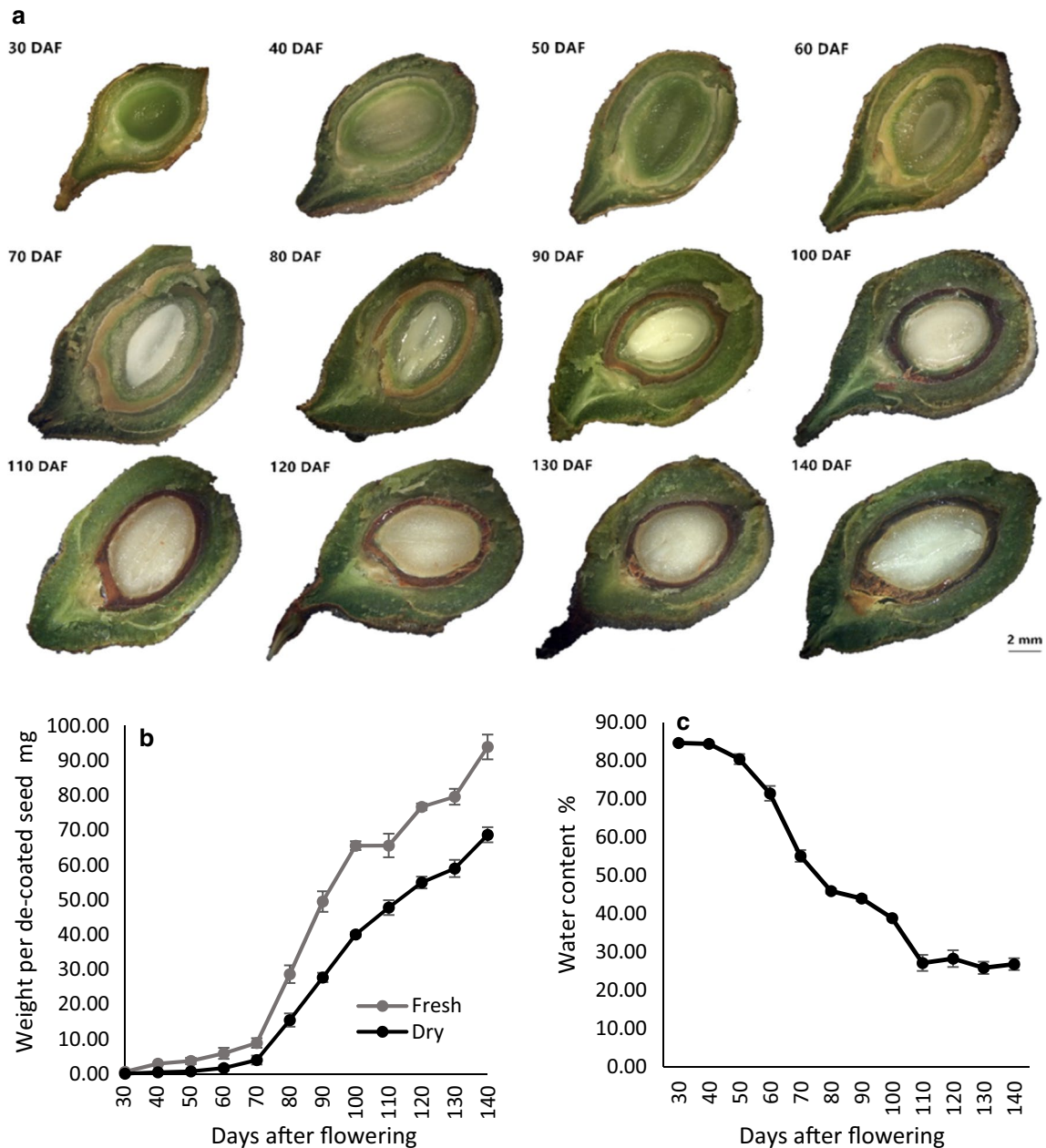


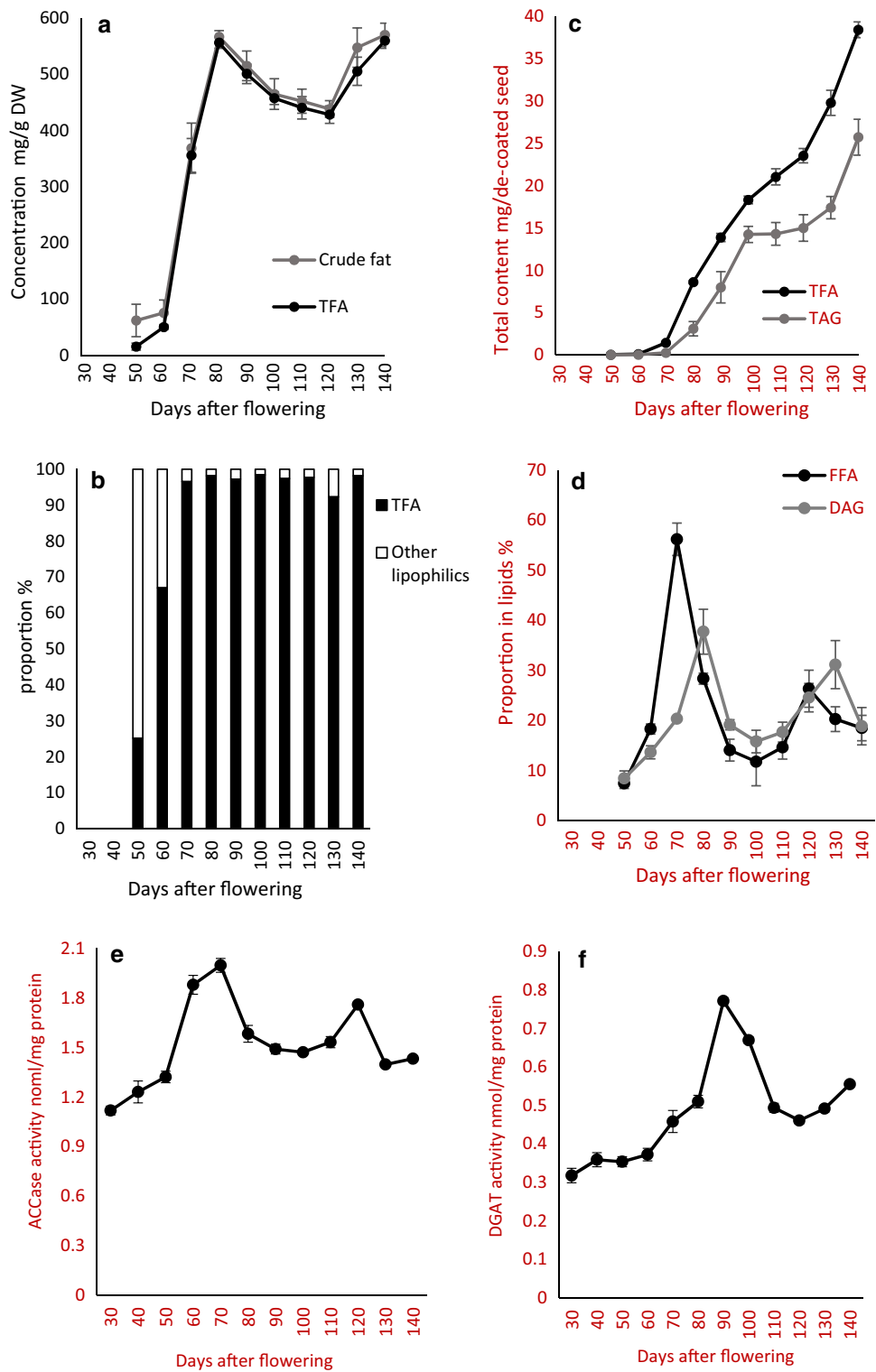
**Fig. 2** Basic biological parameters of *Styrax tonkinensis* maturation dynamics. **a** Photographs show longitudinal sections of fruits at different developmental stages (2.5 $\times$ ). **b** Fresh and dry weight dynamics per kernel. **c** Water content dynamics of de-coated seeds

### Change of carbohydrate content

The concentration of the total soluble sugar was unchanged during the first 10 days and then increased sharply by 67.30% from 40 to 60 DAF (Fig. 4a). It then dropped after 70 DAF to reach a minimum at 110 DAF. The concentration rose steadily again thereafter and reached 127 mg/g on a fresh weight basis at 140 DAF, which was similar to the initial concentration at 30 DAF. Changes in the individual sugars, such as hexoses, fructose, and sucrose, underlay this

pattern (Fig. 4b); however, the fructose and glucose concentrations peaked at 60 and 70 DAF, respectively. The glucose kept a higher concentration level than the fructose for the first 40 days. Sucrose concentrations were considerably lower than the hexose concentrations at around 2 mg/g between 30 and 60 DAF, and then rose gradually to a plateau of 21.87–23.01-mg/g FW after 110 DAF. The hexose-to-sucrose ratio increased progressively between 30 and 60 DAF, and then dropped a dramatic 95% in the following 30 days before stabilizing for the remaining 50 days (Fig. 4c).

**Fig. 3** Lipid synthesis in developing *Styrax tonkinensis* de-coated seeds. **a** Concentration on a dry weight basis of crude fat and total fatty acids (TFA). **b** TFA and other lipophilic substance composition. **c** Total fatty acids and TAG content. **d** Free fatty acids (FFA) and diacylglycerol (DAG) concentration in kernel lipids extracted at different developmental stages. **e** Acetyl coenzyme carboxylase (ACCase) activity dynamics. **f** Diglyceride acyltransferase (DAGT) activity dynamics



The range of glucose/fructose ratio was 1.10–1.27 between 30 and 70 DAF (Fig. 4d); however, the ratio decreased to 0.64 and reached the bottom at 80 DAF. It then raised again and remained quite constant (0.95–1.10) for the last 50 days.

The starch concentration dropped from 3.42- to 1.50-mg/g FW from 30 to 70 DAF (Fig. 4e), while the total amount of starch per kernel varied little. The starch content then rose markedly from 0.013 to 1.092 mg, along with the concentration, over the next 50 days. This

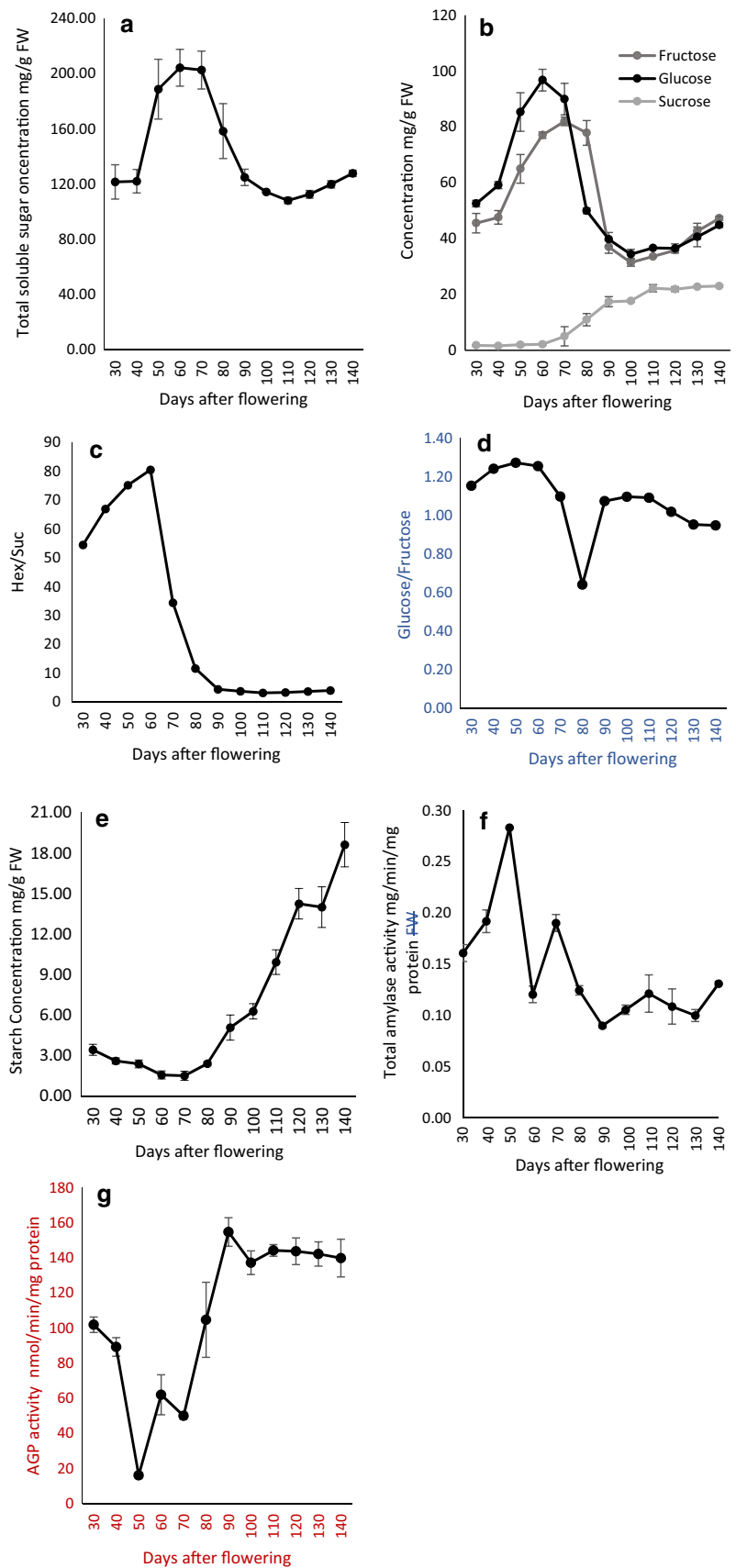
**Table 2** Fatty acids profile dynamics of de-coated *Syzyx tonkinensis* seeds from 50 to 140 days after flowering

	Fatty acids composition (% w/w)													
	50 DAF	60 DAF	70 DAF	80 DAF	90 DAF	100 DAF	110 DAF	120 DAF	130 DAF	140 DAF				
C 24	ND	ND	0.05 ± 0.01	0.04 ± 0.00	0.02 ± 0.00	0.04 ± 0.01	ND	0.08 ± 0.02	0.02 ± 0.01	0.03 ± 0.01				
C 22	ND	ND	0.09 ± 0.01	0.11 ± 0.01	0.07 ± 0.02	0.13 ± 0.03	0.09 ± 0.00	0.22 ± 0.01	0.11 ± 0.02	0.09 ± 0.01				
C 21	ND	ND	ND	ND	0.06 ± 0.02	0.03 ± 0.00	0.05 ± 0.01	0.02 ± 0.00	0.35 ± 0.03	0.03 ± 0.00				
C 20:4	ND	ND	ND	ND	ND	ND	ND	0.20 ± 0.09	0.05 ± 0.02	ND				
C 20:1 (11-Z)	ND	ND	0.12 ± 0.09	0.22 ± 0.00	0.14 ± 0.01	0.30 ± 0.02	0.18 ± 0.02	0.54 ± 0.03	0.33 ± 0.03	0.21 ± 0.06				
C 20	ND	0.30 ± 0.03	0.22 ± 0.02	0.22 ± 0.03	0.12 ± 0.00	0.25 ± 0.06	0.14 ± 0.01	0.52 ± 0.07	0.28 ± 0.03	0.19 ± 0.02				
C 18:3	ND	ND	ND	ND	0.02 ± 0.01	0.08 ± 0.03	0.04 ± 0.02	0.19 ± 0.02	0.03 ± 0.01	ND				
C 18:2 (EE)	ND	ND	ND	0.05 ± 0.01	0.06 ± 0.02	0.09 ± 0.00	0.05 ± 0.02	0.10 ± 0.02	0.03 ± 0.01	0.03 ± 0.01				
C 18:2	22.66 ± 0.22	41.59 ± 1.76	49.39 ± 0.55	54.18 ± 0.17	56.82 ± 0.38	55.30 ± 0.87	56.61 ± 0.79	55.88 ± 2.85	50.75 ± 0.25	51.05 ± 0.31				
C 18:1	17.62 ± 0.11	30.09 ± 0.39	34.84 ± 1.26	30.35 ± 0.27	31.48 ± 0.15	30.23 ± 0.11	31.12 ± 0.44	26.66 ± 0.38	35.38 ± 0.10	36.26 ± 0.27				
Epoxide oleic acid	7.30 ± 0.03	3.10 ± 0.01	0.17 ± 0.00	ND	ND	ND	ND	ND	ND	ND				
C 18	17.42 ± 3.20	6.18 ± 1.03	2.59 ± 0.05	2.37 ± 0.28	1.80 ± 0.11	2.43 ± 0.11	1.93 ± 0.24	3.20 ± 0.24	2.60 ± 0.22	2.29 ± 0.14				
15-methyl-C 17	ND	ND	ND	ND	ND	ND	ND	0.02 ± 0.01	ND	0.01 ± 0.00				
C 17	ND	ND	0.34 ± 0.09	0.44 ± 0.10	0.34 ± 0.02	0.51 ± 0.02	0.30 ± 0.07	0.55 ± 0.01	0.44 ± 0.05	0.30 ± 0.03				
C 16:1	ND	ND	0.10 ± 0.00	0.11 ± 0.01	0.06 ± 0.00	0.13 ± 0.02	0.08 ± 0.02	0.18 ± 0.03	0.05 ± 0.00	0.07 ± 0.01				
C 16:1 (7-Z)	2.26 ± 0.45	1.04 ± 0.01	0.13 ± 0.05	0.13 ± 0.01	0.11 ± 0.00	0.18 ± 0.03	0.08 ± 0.00	0.23 ± 0.01	0.13 ± 0.01	0.10 ± 0.01				
C 16	32.74 ± 3.68	17.70 ± 1.01	11.78 ± 2.13	11.60 ± 0.20	8.78 ± 0.17	10.13 ± 0.43	9.19 ± 0.54	11.23 ± 0.25	9.36 ± 0.93	9.22 ± 0.47				
C 15	ND	ND	ND	ND	ND	0.01 ± 0.00	ND	0.02 ± 0.00	ND	ND				
C 14	ND	ND	0.07 ± 0.00	0.07 ± 0.00	0.05 ± 0.02	0.07 ± 0.02	ND	0.10 ± 0.02	0.02 ± 0.00	0.04 ± 0.00				
C 6	ND	ND	0.10 ± 0.02	0.09 ± 0.02	0.09 ± 0.01	0.11 ± 0.04	0.12 ± 0.00	0.06 ± 0.00	0.07 ± 0.05	0.07 ± 0.01				

ND not-detected, C 24 tetracosanoic acid, C 22 docosanoic acid, C 21 heneicosanoic acid, C 20:4 arachidonic acid, C 20:1 (11-Z) 11-eicosenoic acid (Z)-, C 20 eicosanoic acid, C 18:3 linolenic acid, C 18:2 (EE) 9,12-octadecadienoic acid, (E,E)-, C 18:2, linoleic acid, C 18:1 oleic acid, C 18:1 stearic acid, 15-methyl-C 17 hexadecanoic acid, 15-methyl-, C 17 heptadecanoic acid, C 16:1 palmitoleic acid, C 16:1 (7-Z) 7-hexadecenoic acid, (Z)-, C 16 palmitic acid, C 15 pentadecanoic acid, C 14 tetradecanoic acid, C 6 hexanoic acid



**Fig. 4** Carbohydrate evolution in developing kernels of *Styrax tonkinensis*. **a** Total soluble sugar concentration on a fresh weight basis. **b** Sucrose, glucose, and fructose concentration on a fresh weight basis. **c** Hexose-to-sucrose ratio (calculated from mean concentrations of hexose (glucose + fructose) and sucrose presented in c). **d** Glucose/sucrose ratio. **e** Starch concentration on a fresh weight basis. **f** Total amylase activity dynamics. **g** ADP-glucose pyrophosphorylase (AGP) activity dynamics

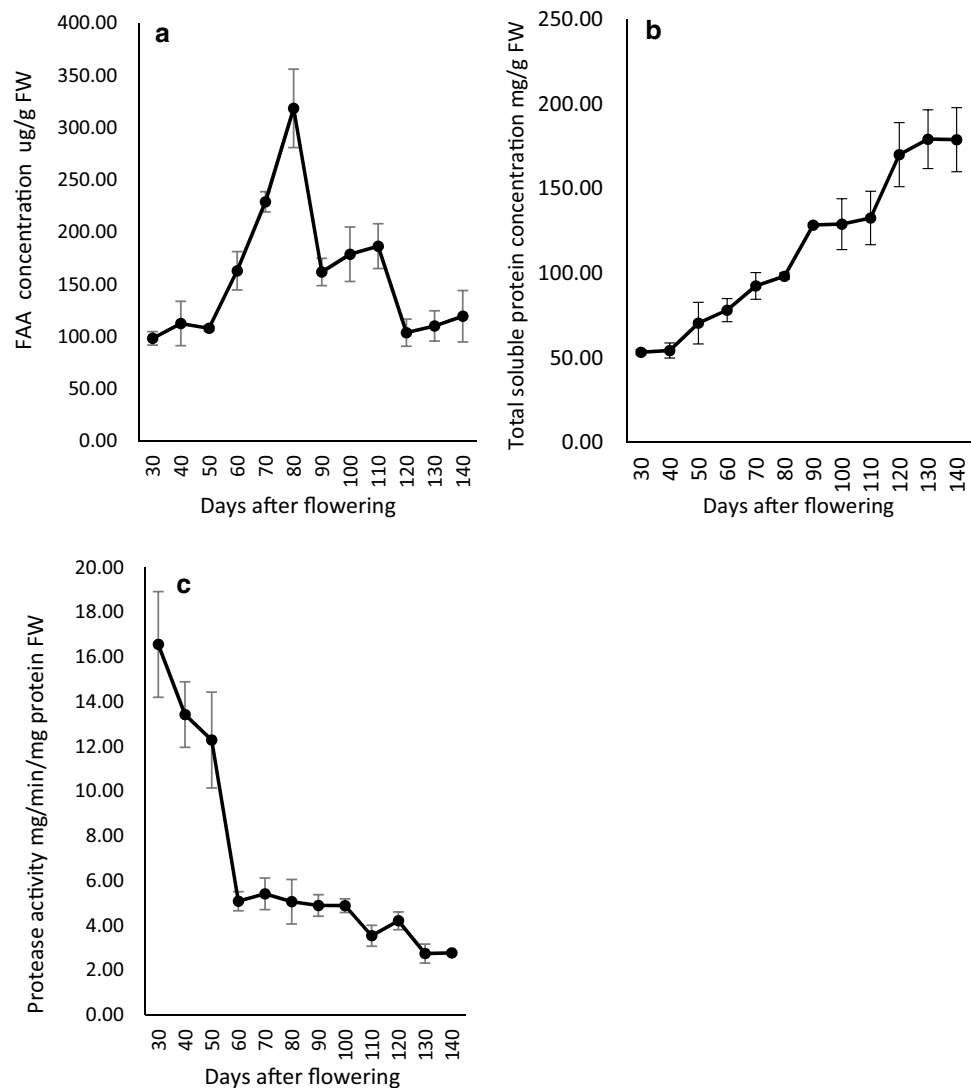


accumulation paused for 10 days before the total starch content rose vigorously and reached 1.747 mg per kernel. The total amylase activity dropped (Fig. 4f), with some fluctuation, over time. Two marked peaks could be observed: the first and higher one at 50 DAF; the second and smaller 70 DAF. The enzyme activity then decreased to between 0.09 and 0.13 mg/(min mg protein). AGP activity remained relatively low between 30 and 70 DAF (Fig. 4g), with an average value of 61.82 nmol/min/mg protein. It then climbed for the next 20 days and peaked at 90 DAF (154.8 nmol/min/mg protein), with a ninefold-increase compared with the lowest activity at 50 DAF. AGP activity then remained stable for the final 40 days, ranging from 142.3 to 144.3 nmol/min/mg protein. A significant negative correlation ( $R = -0.836$ ) between AGP and total amylase was then found.

### Change of amino-acid and soluble protein

The free amino-acid concentration of de-coated benzoin seeds peaked at 80 DAF (Fig. 5a), exceeding 300- $\mu\text{g/g}$  FW. The concentration fell abruptly over the next 10 days, with a 49.15% decrease, followed by a 20-day stationary phase, before the second decline with a similar 44.34% fall between 110 and 120 DAF. The free amino-acid concentration then went into a stationary phase again and stayed below 120  $\mu\text{g/g}$ . Protein accumulation per kernel was slow between 30 and 70 DAF and then sped up. However, the accumulation rate decreased twice, at 90–110 DAF and 120–140 DAF, and soluble protein concentration varied little correspondingly (Fig. 5b), which paralleled the same two stationary phases in free amino-acid concentration. Correlation between the soluble protein and free amino-acid concentration after 80 DAF was significant ( $R = -0.907$ ). Protease activity showed a gradual downward

**Fig. 5** Evolution of free amino acids (FAA) and protein content in developing *Styrax* de-coated seeds. **a** FAA concentration on a fresh weight basis. **b** Protein concentration on a fresh weight basis. **c** Protease activity dynamics



trend with a sharp 58.60% decrease between 50 and 60 DAF (Fig. 5c). In all, there was no evidence indicating net protein hydrolysis in developing seeds over time and the total soluble protein content finally reached 16.79 mg per kernel at 140 DAF.

### Glycooxidation enzymes activities dynamics

The four glycooxidation pathway-related enzyme activities showed profound changes during *S. tonkinensis* seed development, each peaking twice. The PGI, PDHC and MDA activities peaked at 70 DAF (Fig. 6a–c). The PGI activity then dropped linearly and the MDH activity remained at a relatively low level until 110 DAF. The activities of PGI and MDH then both rose suddenly and remarkably to peak again at 120 DAF, with a 148 and 220% increase, respectively, while PDHC activity rose again after 100 DAF until it peaked at 120 DAF as well. The G6PDH activity reached the first peak at 60 DAF and then was subject to a major 17.7% decline in the next 10 days (Fig. 6d). It increased again steadily after 70 DAF to reach a second, higher

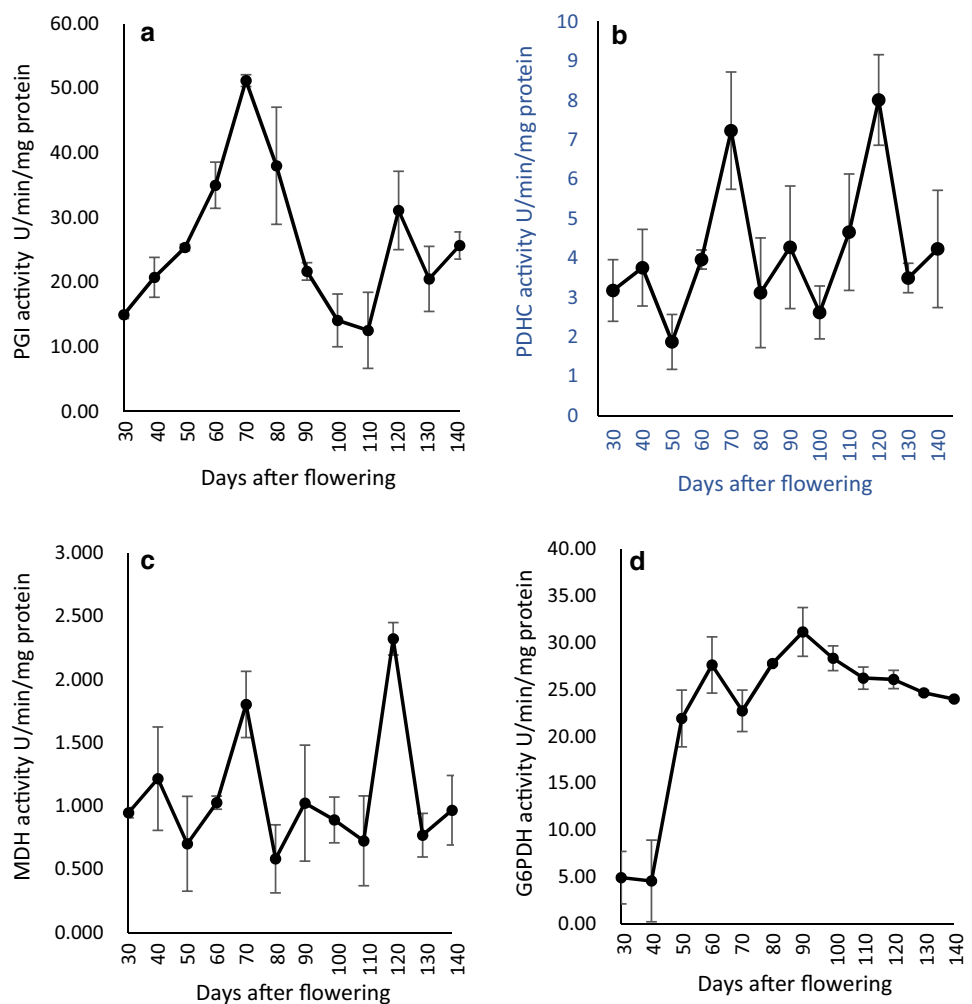
peak at 90 DAF (a 530% increase compared with 30 DAF) before dropping slowly over the final 50 days.

### Discussion

#### Hex/Suc reduction kicks off primary deposition

Increased sucrose flux through developing fruit was believed to result in faster rates of seed filling (Fader and Koller 1985), until Weber et al. (1997) first introduced the hypothesis that a high sucrose against hexose state precedes the phase transition from cell division to storage-associated cell expansion in young legume seeds. This idea was confirmed in *Arabidopsis thaliana* ecotype WS (Baud et al. 2002), and further evidence was obtained from developing seeds of *Arabidopsis* in which the *ap2* mutation caused changes in the ratio of hexose and sucrose, ultimately regulating seed mass (Ohto et al. 2005). Our results in *S. tonkinensis* de-coated seed are consistent with these findings. The variation of glucose, fructose, and sucrose concentration

**Fig. 6** Changes in some respiratory pathway enzyme activities of developing *Styrax tonkinensis* kernels. **a** Phosphoglucose isomerase (PGI), a rise of 0.01 in OD value, represents one unit of PGI activity. **b** Pyruvate dehydrogenase complex (PDHC), a decrease of 1 nmol of 2,6-dichlorophenolindophenol (2,6-DCPIP) in the reaction system, represents one unit of PDHC activity. **c** Malate dehydrogenase (MDH), a drop of 0.1 in OD value, represents one unit of MDH activity. **d** Glucose 6-phosphate dehydrogenase (G6PDH), a drop of 0.01 in OD value, represents one unit of G6PDH activity



levels leads to a dramatic reduction in the hexose/sucrose ratio after 60 DAF (Fig. 4c), which correlated with the abrupt change in size and color of benzoin kernels and the initiation of a rapid increase in kernel dry matter (Fig. 2a, b).

However, the starch accumulation speed (Fig. 4e) stayed relatively low after the Hex/Suc ratio dropped, increasing only 45% between 60 and 70 DAF, compared with the dramatic 16-fold increases in total fatty acids concentration (Fig. 3a). Unlike grains, starch accumulation in benzoin does not have priority. Moreover, the escalating amylase activity (an increase of 58%) and diminishing AGP activity (a decrease of 19%) during the 10 days could be counted as the reasons (Fig. 4f, g). The fructose levels were lower than glucose before 70 DAF (Fig. 4b), which indicates that fructose is the preferred precursor for FA biosynthesis (Hill et al. 2003). Similar data were shown by Chen et al. (2011) in canola seeds. The glucose/fructose ratio (G:F) may be used as a convenient indicator to evaluate the soluble sugar status in plant cells. In this study, G:F ratio dropped from 1.26 to 0.64 between 60 and 80 DAF (Fig. 4d), suggesting the preferential utilization of glucose during the 20 days. However, the down-going G:F ratio was also assumed to be due to the conversion of glucose into fructose, which phosphoglucomutase (PGM) was involved (Wu et al. 2012).

#### Oil accumulation speed slows down (OASD) during seed filling

Storage lipid breakdown during seed maturation has been reported in many species, such as *A. thaliana* seed of WS ecotype (Baud et al. 2002) and oilseed rape (Eastmond and Rawsthorne 2000). Understanding of this peculiarity could help farmers with the harvest timing. In woody oilseed plants, however, the seed development duration is much longer, which could bring more uncertainties to the oil accumulation phase. For benzoin seeds, Shi et al. (2013) were first to find the 30-day decrease in crude lipid concentration, which then they believed that measurement errors were the main reason for this phenomenon. Our results showed that the TFA accumulation was compromised (Fig. 3c); nevertheless, the fatty acid profile remained stable (Table 2), between 80 and 120 DAF, with an average accumulation speed of  $0.37 \text{ mg seed}^{-1} \text{ day}^{-1}$ , which was much slower compared with that between 70 and 80 DAF ( $0.72 \text{ mg seed}^{-1} \text{ day}^{-1}$ ) and 120 and 140 DAF ( $0.74 \text{ mg seed}^{-1} \text{ day}^{-1}$ ). It is noteworthy that, in this study, linolenic acid was hardly detectable in mature benzoin seeds, compared with seeds from Zhejiang (Shi et al. 2013), Fujian and Jiangxi (Fu et al. 2014) provinces, China, suggesting geographic variation in this species.

When we examined the TAG, DAG, and FFA dynamics separately (Fig. 3 c, d), the OASD could be divided into

two phases: 80–100 DAF ( $0.48 \text{ mg seed}^{-1} \text{ day}^{-1}$ ), when TAG accumulation in benzoin seed sped up, with a 362% increase, and FFA and DAG concentration had a severe 58.5% and 58.1% fall respectively; 100–120 DAF ( $0.26 \text{ mg seed}^{-1} \text{ day}^{-1}$ ), when TAG accumulation began to slow down and reach the bottleneck, and FA substrate as well as DAG, the direct TAG precursor, ceased to be consumed and accumulated instead, which might be owing to the “resurgent” ACCase and exhaustion of DGAT activity during the 20 days (Fig. 3e, f). In general, studies with developing seeds indicate that ACCase and DGAT activity associates with lipids synthesis and may catalyze a rate-limiting reaction in fatty acids and TAGs bio-assembly (Jako et al. 2001; Klaus et al. 2004). In this course of study, fact that FFA and DAG concentration climbed after 100 DAF and peaked before TAG synthesis started again indicated the “re-boost” of lipid synthesis system, which was verified by the 19.6% increase in ACCase activity (100–120 DAF) and the 20.5% increase of DGAT activity (120–140 DAF). Overall, our data imply that, during benzoin seed filling, there was a compromised gap in FA synthesis correlating with the TAG accumulation plateau before lipid synthesis recovered again, which is unconventional and differs substantially from what is described previously in tung tree (*Vernicia fordii*)—another oilseed tree species (Cao et al. 2013). The expression level of DGAT1 gene turned high as well in the mid-late stage of *V. fordii* seed maturation. However DGAT2 was the most abundant mRNA in tung seeds from all oil-accumulating stages, with over 10- to 30-fold higher mRNA level compared to DGAT1; Furthermore, this re-rise pattern was not shown in the expression level dynamic of DGAT2. Therefore, it is not surprising that the OASD in benzoin seeds was not shared by tung tree.

#### Carbon diversion from lipid to starch during seed reserve-storing phase

Researchers have established the idea that lipid storage will be influenced by other cell metabolic pathways (Weslake et al. 2009). Between seed starch and oil in particular, as they “stand” respectively upstream and downstream of the glycolytic pathway, evidence that carbon partitioning will eventually tip the starch/oil balance is solid (Lin et al. 2004), and the manipulation to “starve” lipid deposition through up-regulating starch synthesis ability is possible, for both *Abrabidopsis* mutant seeds (Lin et al. 2006) and *Brassica napus* seeds (Boddupalli et al. 1995). Carbon allocation happened after sucrose cleavage and conversion into hexose-phosphates (Klaus et al. 2004). To re-direct carbon into starch synthesis from the fatty acid and lipid deposition, hexoses derived from sucrose need to “avoid” to be converted into acetyl-CoA via glycolysis. In the course of this study, as sucrose-to-lipid conversion occurs

at low rates in benzoin seeds, the enzymatic steps of glycoxidation were shown to have declined activities with a total 75.50% (PGI, Fig. 6a), 35.6% (PDHC, Fig. 6b) and 59.80% (MDH, Fig. 6c) decrease. Furthermore, the start of a rapid starch accumulation period during OASD with a 19-fold higher rate, compared with that of the 50-day duration before (Fig. 4f), could serve as evidence that the carbon consumption priority was shifted towards starch storage for benzoin seeds, which was again verified by facts of a soaring AGP activity (Fig. 4g) and falling ACCase and DGAT activities (Fig. 3e, f). However, G6PDH activity did not coincide with the dropping tendency of PGI, PDHC, and MDH, which indicates the key function of the pentose phosphate pathway during seed development. Similar data is presented by Simcox and Dennis (1978). In this work, G6PDH activity kept dropping at quite a slow rate during the last 50 days (Fig. 6c), which may imply the high activity of G6PDH is not always necessary during lipid accumulation. This assumption is not difficult to be come up with, given the fact that apart from its role as the reducing power provider, G6PDH is also a capable consumer of FA synthesis substrate. This idea is supported by the work of Wakao et al. (2008). The rates of PDHC (1.87–8.00 U/min/mg protein) and MDH (0.73–2.36 U/min/mg protein) activity remained low compared with PGI (14.09–51.18 U/min/mg protein), which could be explained by weak energy flow in the TCA cycle (Schwender et al. 2006). Though hexoses drained from FA synthesis allocated to starch accumulation during OASD in benzoin developing seeds, it was worthy of notice that there were still quite a few DAG left (15.8% of total lipids) at 100 DAF. Plus, in the study, 1% drop of DAG in lipids would correlate a 0.19-mg rise of total TAG content between 80 and 100 DAF. However, TAG stopped to accumulate, until DAG concentration reached 24.6% and DGAT activity recovered after 120 DAF, indicating that TAG synthesis might not start without a certain degree of substrate concentration.

In fact, our study showed the lipid/starch balance tipping could be seen not only during the OASD, but also throughout the benzoin seed filling phase. After the PGI, PDHC, and MDH activities peaked again at 120 DAF, the TFA accumulation speed recovered immediately, correlating with the second upward phase of FFA and DAG concentration, followed by a 10-day lag in starch accumulation. It is worthwhile to note that when FFA concentration dropped after 120 DAF again, starch accumulated at a fast speed accordingly between 130 and 140 DAF; however, the TFA and TAG deposition and rate remained high as well. Therefore, it seems natural to propose that it is the carbon flux trade-off between FFA and starch that was observed during benzoin seed filling in this study. This conclusion may be premature, whereas it is safe to say that TAG synthesis rate was not affected by the starch accumulation, since

fast TAG accumulation and high DGAT activity (80–100 DAF) was observed during OASD, and the post-hoc TAG accumulation plateau between 100 and 120 DAF was more likely caused by insufficient substrate concentration rather than the direct carbon competition with starch biosynthesis. Furthermore, it may suggest that carbon redirection from starch to lipid could not be achieved only by up-regulation of DGAT activity, but also through engineering to boost ACCase activity (Klaus et al. 2004).

### What about protein?

We believe the carbon partitioning between protein and lipid is less obvious. One may argue that the average synthesis rate was high during OASD; nevertheless, there was a slowdown in total protein accumulation present between 90 and 110 DAF, and, furthermore, the protein concentration kept rising all the time when the TFA was accumulating massively before 80 DAF (Fig. 5b). Different patterns in the accumulation of protein and starch were found in this study. Protease activity continuously dropped, negatively correlating with the ever-growing soluble protein concentration ( $R = -0.81$ , Fig. 5c), and two peaks in amylase activity at 50 and 70 DAF correlated with a drop in starch concentration even in the presence of abundant substrates for starch synthesis (glucose and fructose, Fig. 4b). It may be reasonable to consider the protein accumulation as being separate from the starch/oil carbon flux system, given its crucial position during the duration of seed development. However, further evidence does not agree with each other when *AtDGATI* that up-regulates oil deposition was over-expressed in developing rape seeds and resulted in decreases or no effect on protein content (Weselake et al. 2008; Taylor et al. 2009).

The two distinct lag periods (90–110 DAF and 120–140 DAF) in protein concentration dynamics should not be neglected. We do not believe that experimental error can account for that, since the amino-acid time-course changes were parallel with them (Fig. 5a, b). Upon inspection of the dynamic relation between TAG and protein, the two phases were seen to coincide with the time when TAG accumulated rapidly. Further experiments are required to explore the possibility that TAG and protein compete spatially in the endoplasmic reticulum, since they are all synthesized there.

**Author contributions** ZZ is in charge of the designing, finishing most of the experiment, data acquisition and analysis, manuscript preparation, and so on. XW extracted and separate seed lipid by thin layer chromatography. YL is responsible for the accomplishment of experiments about oil and starch synthesis enzyme analysis (acetyl coenzyme carboxylase, diglyceride acyltransferase, and ADP-glucose

pyrophosphorylase activity). FY is critical for important intellectual content and final approval of the version to be published.

**Acknowledgements** The authors acknowledge the funding received from A Project Funded by the Priority Academic Program Development of Jiangsu Higher Education Institutions (PAPD) and the Three New Agricultural Project of Jiangsu Province: Demonstration and Promotion of Effective Nurturing Techniques for *Styrax tonkinensis* as Seedlings and Grown Trees (ZX2014S0020). We would like to thank Mrs. Jia Yu and Mr. Xiaoyue Ji from Advanced Analysis Testing Center, Nanjing Forestry University for the GC-MS technical assistance and Dr. Robert D. Guy from the University of British Columbia for the kind help with the language correction of this paper.

#### Compliance with ethical standards

**Conflict of interest** The authors declare that they have no conflict of interest.

## References

- Baud S, Boutin JP, Miquel M, Lepiniec L, Rochat C (2002) An integrated overview of seed development in *Arabidopsis thaliana* ecotype WS. *Plant Physiol Biochem* 40:151–160
- Bergmeyer HU (1956) *Methods of Enzymatic Analysis*. Second Printing Revised. Verlag Chemie G.m.b.H/Academic press, Weinheim/New York
- Bernfield P (1955) Amylase alpha and beta. In: Colowick SP, Kaplan NO (eds) *Methods in enzymology*, vol 1. Academic press, New York, pp 149–151
- Boddupalli SS, Stark DM, Barry GF, Kishore GM (1995) Effect of overexpressing *ADPGlc* pyrophosphorylase on the oil biosynthesis in canola. *Biochemistry molecular biology plant fatty acids and glycerolipids symposium*. National Plant Lipid Cooperative Symposium, South Lake Tahoe, California
- Bradford MM (1976) A rapid and sensitive method for the quantitation of microgram quantities of protein utilizing the principle of protein-dye binding. *Anal Biochem* 72:248–254
- Brown AP, Wray JL (1968) Correlated changes of some enzyme activities and cofactor and substrate contents of pea cotyledon tissue during germination. *Biochem J* 108:437–444
- Cao H, Shockey JM, Klasson KT, Chapital DC, Mason CB, Schefler BE (2013) Developmental regulation of diacylglycerol acyltransferase family gene expression in tung tree tissues. *PLoS one* 8:e76946
- Chen JM, Qi WC, Wang SY, Guan RZ, Zhang HS (2011) Correlation of Kennedy pathway efficiency with seed oil content of canola (*Brassica napus* L.) lines. *Can J Plant Sci* 91:251–259
- Chen W, Li L, Liu G, Dong Z, Huang Z, Liu H, Chen X and Yu W (2015) Response surface methodology to optimize production of biodiesel from *Styrax tonkinensis*. *Guangzhou Chem Ind* 43:46–49 (in Chinese)
- Eastmond PJ, Rawsthorne S (2000) Coordinate changes in carbon partitioning and plastidial metabolism during the development of oilseed rape embryos. *Plant Physiol* 122(:):767–774
- Emes MJ, Neuhaus HE (1997) Metabolism and transport in non-photosynthetic plastids. *J Exp Bot* 48:1995–2005
- Fader GM, Koller HR (1985) Seed growth rate and carbohydrate pool sizes of the soybean fruit. *Plant Physiol* 79:663–666
- Fu Y, Sun Y, Pan Z, Wang L (2014) Analysis of fatty acids in *Styrax tonkinensis* seed oil by on-line methylation gas chromatography. *Biomass Chem Eng* 48:18–22 (Chinese)
- Gao J (2006) *Experimental guidance for plant physiology*. High Education Press, Beijing (Chinese)
- Hay J, Schwender J (2011) Computational analysis of storage synthesis in developing *Brassica napus* L. (oilseed rape) embryos: flux variability analysis in relation to <sup>13</sup>C metabolic flux analysis. *Plant J* 67:513–525
- Hieu PS, Thuy VH, Thuan PD (2011) Main characteristics of statistical data and the statistical system for wood and wood-processing products in Vietnam. *Small scale For* 10:185–198
- Hill LM, Morley-Smith ER, Rawsthorne S (2003) Metabolism of sugars in the endosperm of developing seeds of oilseed rape. *Plant Physiol* 131(:):228–236
- Jako C, Kumar A, Wei Y, Zou J, Barton DL, Giblin EM, Covello PS, Taylor DC (2001) Seed-specific over-expression of an Arabidopsis cDNA encoding a diacylglycerol acyltransferase enhances seed oil content and seed weight. *Plant Physiol* 126:861–874
- Ke CJ, He YH, He HW, Yang X, Li R, Yuan J (2014) A new spectrophotometric assay for measuring pyruvate dehydrogenase complex activity: a comparative evaluation. *Anal Methods* 6:6381–6388
- Keller GL, Nikolau BJ, Ulrich TH, Wurtele ES (1988) Comparison of starch and ADP-glucose pyrophosphorylase levels in nonembryogenic cells and developing embryos from induced carrot cultures. *Plant Physiol* 86:451–456
- Klaus D, Ohlrogge JB, Neuhaus HE, Dörmann P (2004) Increased fatty acid production in potato by engineering of acetyl-CoA carboxylase. *Planta* 219:389–396
- Li H (2006) *The principles and technologies for plant physiology and biochemistry experiments*. High Education Press, Beijing (Chinese)
- Lin Y, Cluette-Brown JE, Goodman HM (2004) The peroxisome deficient Arabidopsis mutant *ssel* exhibits impaired fatty acid synthesis. *Plant Physiol* 135:814–827
- Lin Y, Ulanov AV, Lozovaya V, Widholm J, Zhang G, Guo J, Goodman HM (2006) Genetic and transgenic perturbations of carbon reserve production in Arabidopsis seeds reveal metabolic interactions of biochemical pathways. *Planta* 225:153–164
- Lowry OH, Rosebrough NJ, Farr AL, Randall RJ (1951) Protein measurement with the Folin phenol reagent. *J Biol Chem* 193:265–275
- McDonald CE, Chen LL (1965) The Lowry modification of the Folin reagent for determination of proteinase activity. *Anal Biochem* 10:175–177
- Morris DL (1948) Quantitative determination of carbohydrates with Dreywood's anthrone reagent. *Science* 107:254–255
- Ohlrogge JB, Browse J (1995) Lipid biosynthesis. *Plant Cell* 7:957–970
- Ohlrogge JB, Jaworski JG (1997) Regulation of fatty acid synthesis. *Annu Rev Plant Biol* 48:109–136
- Ohto MA, Fischer RL, Goldberg RB, Nakamura K, Harada JJ (2005) Control of seed mass by *APETALA2*. *Proc Natl Acad Sci USA* 102:3123–3128
- Pinyopusarerk K (1994) *Styrax tonkinensis*: taxonomy, ecology, silviculture and uses. ACIAR Technical Reports No.31. CPN Publication, Canberra
- Rosen H (1957) A modified ninhydrin colorimetric analysis for amino acids. *Arch Biochem Biophys* 67:10–15
- Schwender J, Shachar-Hill Y, Ohlrogge JB (2006) Mitochondrial metabolism in developing embryos of *Brassica napus*. *J Biol Chem* 281:34040–34047
- Shi C, Li Y, Zhu G, Liu X, Yang L, Sheng W (2013) Seed oil production rate and fatty acid content of *Styrax tonkinensis* during seed maturation. *J Zhejiang Agric For Univ* 30:372–378 (Chinese)

- Shi G, Zhu G, Huang H, Li Y, Liu X, Ye X (2014) Refining and toxicology preliminary evaluation of *Styrax tonkinensis* seed oil. *J Chin Inst Food Sci Technol* 14:192–201 (**Chinese**)
- Simcox PD, Dennis DT (1978) Isoenzymes of the glycolytic and pentose phosphate pathways in proplastids from the developing endosperm of *Ricinis communis* L. *Plant Physiol* 61:871–877
- Simcox PD, Garland W, Deluca V, Canvin DT, Dennis DT (1979) Respiratory pathways and fat synthesis in the developing castor oil seed. *Can J Bot* 57:1008–1014
- Taylor DC, Zhang Y, Kumar A, Francis T, Giblin EM, Barton DL, Ferrie JR, Laroche A, Shah S, Zhu W, Snyder CL (2009) Molecular modification of triacylglycerol accumulation by over-expression of *DGATI* to produce canola with increased seed oil content under field conditions. *Botany* 87:533–543
- Wakao S, Andre C, Benning C (2008) Functional analyses of cytosolic glucose-6-phosphate dehydrogenases and their contribution to seed oil accumulation in *Arabidopsis*. *Plant Physiol* 146:277–288
- Weber H, Borisjuk L, Wobus U (1997) Sugar import and metabolism during seed development. *Trends Plant Sci* 5:169–174
- Weselake RJ, Taylor DC, Rahman MH, Shah S, Laroche A, McVetty PB, Harwood JL (2009) Increasing the flow of carbon into seed oil. *Biotechnol Adv* 27:866–878
- Wu BH, Quilot B, Génard M, Li SH, Zhao JB, Yang J, Wang YQ (2012) Application of a SUGAR model to analyse sugar accumulation in peach cultivars that differ in glucose–fructose ratio. *J Agric Sci* 150:53–63
- Xu L, Yu F (2015) Corolla structure and fragrance components in *Styrax tonkinensis*. *Trees Struct Funct* 29:1127–1134
- Yokoyama S (2004) Forest, ethnicity and settlement in the mountainous area of Northern Laos. *Southeast Asian Stud* 42:132–156
- Yoshida H, Shigezaki J, Takagi S, Kajimoto G (1995) Variations in the composition of various acyl lipids, tocopherols and lignans in sesame seed oils roasted in a microwave oven. *J Sci Food Agric* 68:407–415
- Yoshida H, Shougaki Y, Hirakawa Y, Tomiyama Y, Mizushima Y (2004) Lipid classes, fatty acid composition and triacylglycerol molecular species in the kernels of pumpkin (*Cucurbita* spp.) seeds. *J Sci Food Agric* 84:158–163
- Yoshida H, Tanigawa T, Kuriyama I, Yoshida N, Tomiyama Y, Mizushima Y (2011) Variation in fatty acid distribution of different acyl lipids in rice (*Oryza sativa* L.) brans. *Nutrients* 3:505–514
- Yu, Zhang (1999) The determination of soluble sugar in plant tissues. In: Shanghai Institute of Plant Physiology, CAS and Shanghai Society of Plant Physiology (eds) *Experimental guidance for modern plant physiology*. Science Press, Beijing, pp 127–128 (**Chinese**)